Accepted Manuscript

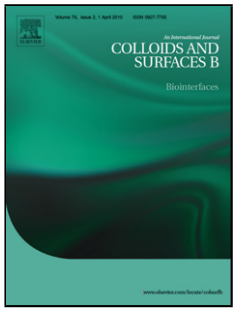

Title: Superoxide dismutase in nanoarchaeosomes for targeted delivery to inflammatory macrophages

Authors: Priscila Schilrreff, Yamila Roxana Simioni, Horacio Emanuel Jerez, Ayelen Tatiana Caimi, Marcelo Alexandre de Farias, Rodrigo Villares Portugal, Eder Lilia Romero, Maria Jose Morilla

PII: S0927-7765(19)30210-3
DOI: https://doi.org/10.1016/j.colsurfb.2019.03.061
Reference: COLSUB 10111

To appear in: *Colloids and Surfaces B: Biointerfaces*

Received date: 12 January 2019
Revised date: 14 March 2019
Accepted date: 27 March 2019

Please cite this article as: Schilrreff P, Simioni YR, Jerez HE, Caimi AT, de Farias MA, Villares Portugal R, Romero EL, Morilla MJ, Superoxide dismutase in nanoarchaeosomes for targeted delivery to inflammatory macrophages, *Colloids and Surfaces B: Biointerfaces* (2019), https://doi.org/10.1016/j.colsurfb.2019.03.061

Superoxide dismutase in nanoarchaeosomes for targeted delivery to inflammatory macrophages

Priscila Schilrreff[1], Yamila Roxana Simioni[1], Horacio Emanuel Jerez[1], Ayelen Tatiana Caimi[1], Marcelo Alexandre de Farias[2], Rodrigo Villares Portugal[2], Eder Lilia Romero[1] and Maria Jose Morilla[1,*]

[1] Nanomedicine Research & Development Center, Departamento de Ciencia y Tecnología, Universidad Nacional de Quilmes. Roque Saenz Peña 352, Bernal, B1876BXD, Argentina.

[2] Brazilian Nanotechnology National Laboratory, CNPEM, Caixa Postal 6192, CEP 13.083-970, Campinas, São Paulo, Brazil.

***** Corresponding author

Maria Jose Morilla

Nanomedicine Research & Development Center, Departamento de Ciencia y Tecnología, Universidad Nacional de Quilmes. Roque Saenz Peña 352, Bernal, B1876 BXD

Tel +541143657100

Fax +541143657132

email: jmorilla@unq.edu.ar

Statistical summary:

Total number of words: 5999

Tables: 1

Figures: 7

Supplementary figures: 4

Graphical abstract

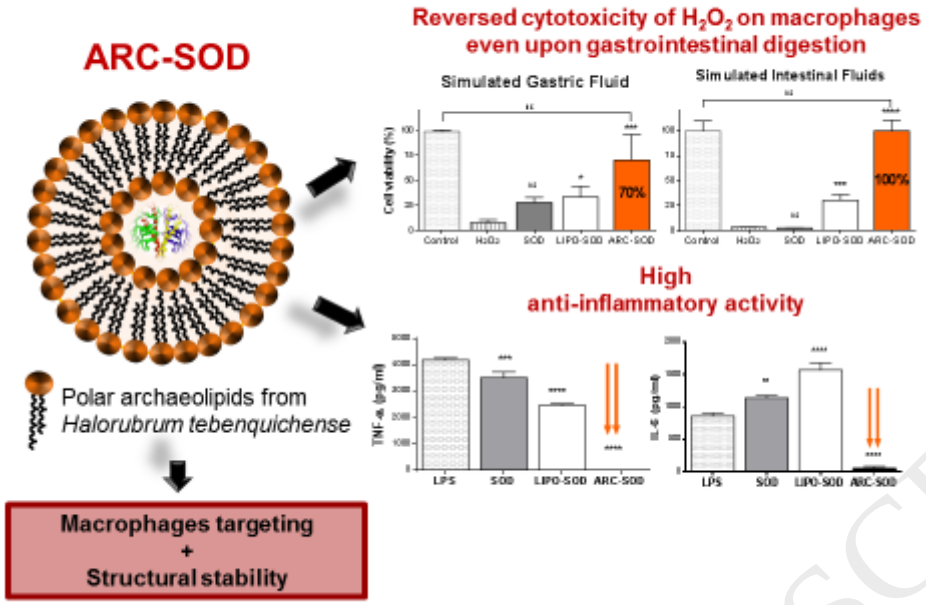

Highlights

- -ARC protect SOD from gastrointestinal digestion
- -ARC-SOD are highly uptaken by macrophages
- -ARC-SOD reverse the cytotoxic effect of H_2O_2 and intracellular ROS on macrophages
- -ARC-SOD suppress IL-6 and TNF-α release on stimulated macrophages

Abstract

Oxidative stress plays an essential role in the pathogenesis and progression of inflammatory bowel disease. Co-administration of antioxidants and anti-inflammatory drugs has shown clinical benefits. Due to its significant reactive oxygen species (ROS) scavenging ability, great interest has been focused on superoxide dismutase (SOD) for therapeutic use. However, oral SOD is exposed to biochemical degradation along gastrointestinal transit. Furthermore, the antioxidant activity of SOD must be achieved intracellularly, therefore its cell entry requires endocytic mediating mechanisms. In this work, SOD was loaded into nanoarchaeosomes (ARC-SOD), nanovesicles fully made of *sn* 2,3 ether linked phytanyl saturated archaeolipids to protect and target SOD to inflammatory macrophages upon oral administration. Antioxidant and anti-inflammatory activities of ARC-SOD, non-digested and digested in simulated gastrointestinal fluids, on macrophages stimulated with H_2O_2 and lipopolysaccharide were determined and compared with those of free SOD and SOD encapsulated into highly stable liposomes (LIPO-SOD).

Compared to SOD and LIPO-SOD, ARC-SOD (170 ± 14 nm, -30 ± 4 mV zeta potential, 122 mg protein/g phospholipids) showed the highest antioxidant and anti-inflammatory activity: it reversed the cytotoxic effect of H_2O_2, decreased intracellular ROS and completely suppressed the production of IL-6 and TNF-α on stimulated J774A.1 cells. Moreover, while the activity of LIPO-SOD was lost upon preparation, gastrointestinal digestion and storage, ARC-SOD was easy to prepare and retained its antioxidant capacity upon digestion in simulated gastrointestinal fluids and after 5 months of storage. Because of their structural and pharmacodynamic features, ARC-SOD may be suitable for oral targeted delivery of SOD to inflamed mucosa.

Keywords: gastrointestinal stability; reactive oxygen species; inflammatory bowel diseases

1. Introduction

Clinical benefits of co-administration of anti-inflammatory drugs and antioxidants for inflammatory bowel disease (IBD) patients have recently been recognized [1-3]. In particular, antioxidant enzymes are known to display higher efficacy than non-enzymatic antioxidants [4]. Specifically, the main function of superoxide dismutase (SOD) is neutralizing superoxide anions ($^*O_2^-$), that are precursors of all other more toxic reactive oxide species (ROS) and reactive nitrogen species (RNS). However, despite of the great interest raised by its significant ROS scavenging ability, several drawbacks limits its clinical use [5-8]. One of them is SOD´s lability upon oral administration, where SOD is degraded by proteolysis [9]. Another limitation is its high molecular weight (32 KDa, for the cytoplasmic dimeric Cu/Zn form called SOD1), that impairs its diffusion to the cell cytoplasm where superoxide anions are produced [10]. It has been shown also that upon intravenous administration, SOD is rapidly eliminated by renal clearance with a half-life of only a few minutes (6-10 min) [11, 12]. Attempting to modify its pharmacokinetics and biodistribution, SOD has been encapsulated in liposomes for local mucosal administration [13], conjugated to phosphatidylcholine (PC-SOD) for intravenous administration [14] and only recently, conjugated to an O-(2-hydroxyl)propyl-3-trimethylammonium chitosan chloride derivative for oral administration [15]. In spite that a phase II clinical study showed that intravenous PC-SOD injected once daily for 4 weeks significantly improved the disease activity index scores of ulcerative colitis patients [16], the parenteral administration of macromolecular antioxidants does not seem to be a realistic option to treat patients over prolonged periods, that in IBD may be extended for life. Moreover, of displaying unnecessary systemic antioxidant effects, infusions of exogenous proteins are known to induce potentially lethal acute hypersensitivity reactions [17-19].

Instead, SOD could be orally administered if loaded in targeted-to-inflamed macrophages nanoparticulate carriers aimed to protect it from the gastrointestinal (GI) harsh conditions. In this way, the cellular uptake and subsequent cytoplasmic delivery of SOD would be facilitated. Besides, SOD activity would be limited to inflamed mucosa, constituting an attractive option to increase the efficacy of current standard IBD treatments. Archaebacterias on the other hand, are known to possesses archaeolipids, lipids having unique chemical nature made of saturated isoprenoid chains linked via ether bonds to the glycerol carbons at the *sn* 2,3 position. Different to liposomes prepared with phospholipids from plants or animal sources, ARC are colloidal and chemically resistant to different stress such as heat sterilization, storage under cold-free conditions [20] and nebulization [21]. Importantly, ARC are stable under GI conditions and efficiently protect encapsulated proteins from digestion [22]; concomitantly, shells made of archaeolipids layer protect solid lipid nanoparticles from lipolysis [23]. Another interesting property is the natural targeting ability of certain ARC, that depends on the type of lipids produced by different archaebacteria gender [24]. Specifically, ARC made of archaeolipids from *Halorubrum tebenquichense* contain PGP-Me, a ligand for scavenger receptors class A (SRA1) [25] highly expressed on macrophages and dendritic cells. Such naturally targeted ARC thus, facilitate the endocytic uptake of carried payload by macrophages with no aid of complex chemical derivatization [26, 27].

In this work therefore, SOD loaded into unique lipid vesicles (nanoarchaeosomes, ARC) made of lipids extracted from the hyperhalophilic archaebacteria *H. tebenquichense* (ARC-SOD), were prepared and characterized. Antioxidant and anti-inflammatory activity of ARC-SOD non-digested and digested in simulated gastric and intestinal fluids, on macrophages stimulated with H_2O_2 or lipopolysaccharides (LPS), were determined by MTT assay, ROS production and proinflammatory cytokines release, respectively. Results were compared with a suspension of SOD in buffer and SOD loaded into highly stable liposomes made of HSPC: cholesterol 3:2 molar ratio (LIPO-SOD).

2. Materials and methods

2.1 Materials

Soybean phosphatidylcholine (SPC, purity >90%) was a gift from Lipoid, Ludwigshafen, Germany. Hydrogenated soy phosphatidylcholine (HSPC) was obtained from Northern Lipids Inc. (Vancouver, Canada). 3-(4,5-Dimethyl-2-thiazolyl)-2,5-diphenyl-2H-tetrazolium bromide (MTT), Lipopolysaccharide from *Escherichia coli* 0111:B4, pepsin, superoxide dismutase from bovine erythrocytes, Laurdan, Sephacryl S-200 and pyrogallol were purchased from Sigma-Aldrich (Buenos Aires, Argentina). Sodium dodecyl sulphate (SDS) was supplied by ICN Biomedicals (Irvine, CA, USA). Cholesterol was purchased from ICN Biomedicals Inc. (Aurora, Ohio). Superoxide dismutase was obtained from SOD nutritional supplement Douglas

Laboratories (USA). Porcine pancreatic lipase was a gift from Gador Argentina (Biozym). Lissamine™ rhodamine B 1,2-dihexadecanoyl-sn-glycero-3-phosphoethanolamine, triethylammonium salt (RhPE) was purchased from Thermo Fisher Scientific, MA, USA. 5-(and-6)-chloromethyl-2′,7′-dichlorodihydrofluorescein diacetate, acetylester (carboxy-H2DCFDA) was from Molecular Probes, Oregon, USA.

Roswell Park Memorial Institute (RPMI) 1640 Medium, Minimum Essential Medium (MEM), supplements L-glutamine, pyruvate, antibiotic/antimycotic and trypsin were from where from Gibco, Argentina. Fetal bovine serum (FBS) was from Internegocios SA (Buenos Aires, Argentina). Hydrogen peroxide (H_2O_2) was from Parafarm (Buenos Aires, Argentina). Tritón X-100 was from Biopack. Other reagents used were of analytical grade and were acquired from Anedra, Argentina.

2.2 Archaebacteria growth, extraction, and characterization of total polar archaeolipids

H. tebenquichense archaea were grown using a 25 L home-made stainless-steel bioreactor in basal medium supplemented with yeast extract and glucose at 37°C. Total polar archaeolipids (TPA) were extracted from biomass using the Bligh and Dyer method modified for extreme halophiles [28]. The reproducibility of each TPA-extract composition was routinely screened by phosphate content [29], and electrospray-ionization mass spectrometry, as described by [30].

2.3 Obtention and characterization of SOD suspension

Aqueous suspension of the content of capsules were prepared at 50 mg/ml in citrate buffer 10 mM plus 0.145 M NaCl pH 5.6 (citrate buffer). Suspension was centrifuged at 1800 g for 10 min, and the supernatant was analysed by protein content as state in section 2.5.1, by enzymatic activity as state in section 2.5.2, by UV-vis spectrum from 200 to 600 nm in a Shimadzu 1603 spectrum, and by electrophoresis. Aliquot of suspension containing 0.03-0.06 mg protein was run by electrophoresis in 15% sodium dodecyl sulfate-polyacrylamide gels (SDS-PAGE). Briefly, the samples were mixed with 0.21 M Tris-HCl pH 6.8, 20% w/v SDS. Proteins were separated at a constant voltage of 200 V, using 25 µM Tris, 192 µM glycine pH 8.3 as running buffer. The staining was performed with Coomassie Brilliant Blue R-250 10 % w/v in 40% v/v ethanol. Molecular marker of Bio-Rad 2-D (MW: 17.500 -76.000 Da) was used as molecular weight standard.

2.4 Preparation of SOD-nanovesicles (ARC-SOD and LIPO-SOD)

ARC loaded with SOD ARC (ARC-SOD, made of TPA) and liposomes loaded with SOD (LIPO-SOD; made of HSPC: cholesterol 3:2 mol:mol) were prepared by the thin film hydration method followed by extrusion. Briefly, mixtures of lipids were dissolved in chloroform:methanol 1:1 v/v were mixed in round bottom flasks and then rotary evaporated at 40°C until elimination into . The lipid films were flushed with N_2 and hydrated with 7.5 mg/ml SOD in citrate buffer up to a final concentration of 20 mg/ml total lipids. Then suspensions were extruded 15 times through a sandwich of 0.8 µm and 0.2 µm pore-size polycarbonate membranes using a Thermobarrel extruder (Northern Lipids, Vancouver, Canada). For LIPO-SOD preparation, hydration and extrusion was carried out at 55-60ºC. Free SOD was removed from SOD-nanovesicles by gel filtration on Sephacryl S-200 using the mini column centrifugation technique [31].

To prepare Rh-PE-labelled nanovesicles (RhPE-ARC and RhPE-LIPO), Rh-PE (a fluorescent hydrophobic tracer) was added at 0.5% weight to phospholipids.

2.5 Characterization of nanovesicles

2.5.1 Quantification of phospholipids and proteins

Phospholipids were quantified by a colorimetric phosphate microassay [29]. Proteins were quantified by BCA assay using a commercial kit (Micro BCATM Protein Assay Kit, Thermo Scientific) after complete disruption of nanovesicles with SDS 5% v/v final concentration (30 min incubation at room temperature).

2.5.2 Enzymatic activity

SOD activity was performed by pyrogallol autoxidation method as described by Zhao et. al. 2017 [15]. The method is based on the capacity of SOD to inhibit the autooxidation of pyrogallol by competing with $*O_2^-$ in alkaline solution and in the presence of EDTA.

Briefly, an aliquot of 25 µl of fresh solution of 50 mM pyrogallol in 10 mM HCl was mixed with 200 µl of SOD suspensions and thoroughly mixed with an appropriate volume of 50 mM Tris-

HCl buffer pH 8.2 containing 1 mM Na_2EDTA to a final volume of 1 ml. The spectrum (200-700 nm) of the mixture was measured every 40-50 s for 5 min and the absorbance at 320 nm was registered. LIPO-SOD and ARC-SOD suspensions were previously concentrated twice in Savant SpeedVac Concentrator at room temperature and SOD was release after complete disruption of nanovesicles with Tritón X-100 (final concentration 10% v/v).

The percentage of inhibition of autooxidation of pyrogallol (I%) was calculated using the following formula: $[(\Delta A320c/t-\Delta A320s/t)/\Delta A320c/t] \times 100$. Where $\Delta A320c/t$ is the change in absorbance at 320 nm between 0 and 5 min of control (pyrogallol alone) and $\Delta A320s/t$ is the change in absorbance at 320 nm between 0 and 5 min of sample (pyrogallol plus SOD).

2.5.3 Size and zeta potential

Size and zeta potential were determined by dynamic light scattering (DLS) and phase analysis light scattering (PALS) respectively, using a nanoZsizer apparatus (Malvern Instruments, Malvern, United Kingdom). Samples were diluted 1 to 20 in citrate buffer.

2.5.4 Morphology by Cryo-Transmission Electron microscopy (Cryo-TEM)

Samples were prepared in a controlled environment vitrification system, equilibrated at 22°C and analyzed using a TALOS F200C (Thermo Fischer Scientific, USA) electron microscope operating at 200 kV. Images were acquired using a Ceta 16M 4k x 4k pixels CMOS camera (Thermo Fischer Scientific, USA). Sample preparation and data acquisition were performed at the Electron Microscopy Laboratory (LME)/Brazilian Nanotechnology National Laboratory (LNNano).

2.5.5 Laurdan generalized polarization (GP) and fluorescence anisotropy (FA)

The order and fluidity of nanovesicles bilayers were assessed by determining GP and FA of Laurdan respectively, according to [25]. Briefly, nanovesicles were labelled with Laurdan by mixing 10 μl of 120 mM Laurdan in methanol with a volume of nanovesicles sufficient to render a 1:20 mol:mol Laurdan:lipids ratio. Measurements were carried out with a fluorescence spectrometer *LS 55, PerkinElmer.*

GP was calculated using the following equation: $GP = I_{440} - I_{490} / I_{440} + I_{490}$.

Where I_{440} and I_{490} are the fluorescence intensities at λ_{em}=440 nm and λ_{em}=490 nm respectively, obtained from the spectra between 400-600 nm at λ_{ex}=364nm ($Slit_{ex}$: 5.0 nm and $Slit_{em}$: 5.0 nm. Scan Speed: 100 nm/min)

FA was calculated by the fluorimeter software according to the following equation: $FA = (I_0 - G\, I_{90}) / (I_0 + 2G\, I_{90})$.

Where I_0 and I_{90} are the fluorescence intensities at λ_{em}=440 nm with λ_{ex}=364 nm and the excitation polarizer oriented at 0 and 90° respectively. The correction factor (G) was obtained from the ratio of emission intensity at 0 and 90° with the excitation polarizer oriented at 90° (after subtraction of scattered light).

2.6 Cell lines and culture

Immortalized murine macrophages J774A.1 (ATCC® TIB-67™) were supplied by Dra. Erina Petrera, Facultad de Ciencias Exactas y Naturales, Universidad Nacional de Buenos Aires, Argentina. Caco-2 cells were kindly provided by Dr. Guillermo Docena, Instituto de Estudios Inmunológicos y Fisiopatológicos IIFP, Universidad Nacional de La Plata, Argentina. J774A.1 cells were maintained in RMPI 1640 and Caco-2 cells were maintained in MEM with 1% pyruvate both supplemented with 10% FBS, 100 U/ml penicillin 100 μg/ml streptomycin and 2 mM L-glutamine in a humidified atmosphere of 5% CO_2 at 37°C.

2.7 Cytotoxicity on macrophages and enterocytes

Cell viability upon incubation with SOD and SOD-nanovesicles was measured by MTT assay. Briefly, J774A.1 and Caco-2 cells were seeded in 96-well plates at a density of 4×10^4 cells per well and grown for 24 h. Then, cells were incubated with 200 μl of different concentration samples diluted in a fresh medium with 5% FBS. The concentrations for nanovesicles formulations were 2, 0.8, 0.5, and 0.2 mM phospholipids (PL) and the corresponding SOD concentration were 8, 3, 1.5 and 0.8 μM. After 5 or 24 h of incubation (with the highest concentration) cells were washed with PBS and 100 μl of 5 mg/ml MTT was added to each well. After 3 h of incubation, MTT solution was removed, insoluble formazan crystals were dissolved in dimethyl sulfoxide, and absorbance was measured at 570 nm in a microplate

reader (Cytation 5 BioTeck, Winooski, VT, USA). Cell viability was expressed as a percentage of control cells grown in culture medium.

2.8 Uptake by macrophages

The uptake of RhPE labelled nanovesicles were measured by flow cytometry. Briefly, J774A.1, were seeded on 24-wells culture plates at a density of 1.5 x 10^5 cells per well and grown for 24 h. Then, cells were incubated with 0.1 mg/ml RhPE-ARC and RhPE-LIPO in complete medium for different times (1 and 5 h) at 37°C. After incubation, the cells were trypsinized, washed with PBS and a total of 1×10^4 cells were analyzed by flow cytometry (BD FACSCalibur TM; BD Biosciences, CA, USA).

2.9 Protective effect against oxidative damage induced by H_2O_2 on J774.A1 cells

2.9.1 Concentration of H_2O_2 that reduced 50% of J774.A1 cells viability

H_2O_2 was used as oxidative stress inductor on macrophages. For that aim, the concentration of H_2O_2 that reduced ~ 50 % viability of J774.A1 cells by MTT assay upon 1 h of incubation was found. Briefly, J774A.1 cells were seeded in 96-well plates at a density of 4 x 10^4 cells per well and grown for 24 h. Then, cells were incubated with 200 µl of different concentration of H_2O_2 ranging from 1 mM to 0.01 µM diluted in fresh medium with 5% FBS. After 1 h of incubation cells were washed with PBS and viability was measured by MTT as described in section 2.7

2.9.2 Protective effect of SOD-nanovesicles

The protective effect of SOD and SOD-nanovesicles on oxidized J774.A1 cells was measured as the capacity of induced survival by MTT assay. Briefly, J774.A1 cells were treated with 1 mM de H_2O_2 as stated in section 2.9.1. Upon 1 h of incubation, the medium was removed, cells were washed with PBS and fresh medium containing ARC-SOD, LIPO-SOD and SOD at 2 mM PL-8 µM SOD was added. Upon 5h and 24 h of incubation, medium was removed, and viability was measured by MTT as described in section 2.7.

2.10 Inhibition of reactive oxygen species (ROS) generation

J774.A1 cells were seeded at a density of 2 ×10^5 cells per well onto 24-well plates and grown for 24 h at 37°C. Then, the medium was replaced by fresh medium with 5% FBS containing SOD or SOD-nanovesicles with 1 µg/ml LPS. LPS- stimulated and non-stimulated cells without treatments were used as positive and negative controls, respectively. After 24 h of incubation at 37°C, medium was removed, and cells were incubated with 13 µM H_2DCFDA for 30 min at 37°C. After incubation, the cells were trypsinized, washed with PBS and a total of 1×10^5cells were analysed by flow cytometry (λEx/Em: ~492–495/517–527 nm). Data were analysed using WinMDI 2.9 software (Microsoft, Redmond, WA, USA).

2.11 *In vitro* anti-inflammatory activity

The *in vitro* anti-inflammatory activity of SOD and SOD-nanovesicles was determined by measuring the release of proinflammatory cytokines by cells stimulated with LPS. Briefly, J774.A1 were seeded at a density of 4 x 10^4 cells per well onto 96 well plates and grown for 24 h at 37°C. Then cells were co-incubated with 1 µg/ml LPS and SOD, ARC-SOD or LIPO-SOD at 2 mM PL-8 µM SOD. After 24 h of incubation at 37°C, supernatants were collected and stored at -20°C until analysis. Mouse TNF-α and IL-6 levels were measured by enzyme-linked immune sorbent assay (BD OptEIA™, BD Biosciences) following the manufacturer's instructions. Absorbance measurements were carried out at 450 nm on a microplate reader.

2.12 Stability under gastrointestinal conditions

To assess for the stability of SOD and SOD-nanovesicles upon digestion, simulated gastric fluid (SGF) and simulated intestinal fluid (SIF) were prepared. SGF which contained 3.2 mg/ ml pepsin and 34.2 mM NaCl at pH 1.2 were prepared according to USP specifications (Test Solutions, United States Pharmacopeia 35, NF 30, 2012). On the other hand, simulated intestinal fluid (SIF), which contained 150 mM NaCl, 5 mM $CaCl_2$, 5 mM sodium taurocholate, 1 mg/ml SPC, 300 UI/ml porcine pancreatic lipase and 0.5% SDS buffered at pH 6.8 with Tris-HCl 10 mM was prepared [32].

Then, 0.1 ml of SOD and SOD-nanovesicles were diluted with 0.9 ml of SGF and incubated at 37°C in an orbital shaker at 190 rpm for 30 min. On the other hand, 0.1 ml of SOD or

nanovesicles were diluted with 0.9 ml of SIF and incubated at 37 °C in an orbital shaker at 190 rpm for 2 h. After SGF and SIF incubations the samples were centrifuged for 1 min at 15000 g to remove pancreatic aggregates from the fluid. The particle size, polydispersity index and zeta potential after incubation were determined as stated above.

Next digested samples were separate from SGF or SIF by size exclusion chromatography with sephacryl S-200 matrix and then concentrated 2 times in a Savant SpeedVac Concentrator at room temperature. The concentration of lipids and proteins was quantified as described in section 2.5.1. The SGF and SIF digested SOD and SOD-nanovesicles were used for incubation with H_2O_2 oxidized J774.A1 cells along 5 h and 24 h and then processed for MTT analysis as state in section 2.9.2.

2.13 Colloidal stability at acidic pH and sodium cholate

ARC-SOD and LIPO-SOD at equivalent SOD concentration of 1 mg/ml were dissolved separately in citrate buffer with varying pH levels (pH 1, 2, 3, 4 and 5) and allowed to incubate at room temperature for 1 h. In a similar way, ARC and LIPO were incubated with increasing concentrations of NaChol for 1 h. The particle size, polydispersity index and zeta potential after incubation were determined as stated above. Besides, enzymatic activity of SOD, ARC-SOD and LIPO-SOD after incubation for 1 h at pH 1.2 and 37 °C was measured as stated in section 2.5.2.

2.14 Stability upon storage

The colloidal stability of LIPO-SOD and ARC-SOD were determined after 5 months stored at 4ºC. Nanoparticle size and zeta potential before and after storage were determined as stated before, while enzymatic activity was measured as state in section 2.5.2.

2.15 Statistical analysis

The results are presented as mean ± S.D. One-way ANOVA Dunnett's or Tukey's multiple comparisons test was performed using Prisma 6.00 software (GraphPad Software Corporation, San Diego, California, USA) to assess the significance of the differences between the data. Differences were considered significant at *$p < 0.05$; **$p < 0.01$; ***$p < 0.001$ and ****$p < 0.0001$; ns: represents not significant ($p > 0.05$).

3. Results

3.1 SOD-nanovesicles structure

SOD was obtained from the nutritional supplement *S.O.D.* of Douglas Laboratories. Each capsule contains Cu/Zn SOD from porcine liver extract formulated with microcrystalline cellulose, jelly and magnesium stearate. A suspension of SOD was prepared by solubilizing the given mass in citrate buffer and removing the insoluble excipients by centrifugation. The suspension of 7.5 ± 2.4 mg/ml of proteins showed a peak of maximum absorbance at 258 nm due to phenylalanine, at 680 nm due to the Cu chromophore of SOD1 as well as absence of the 280 nm peak, coincident with the absence of tryptophan in SOD [33]. Moreover, the SDS-PAGE showed a unique band of 33000 Da, in coincidence with the band of standard SOD, displaying 77 % of enzyme activity, measured as inhibition of pyrogallol autooxidation/mg protein.

SOD suspension (isoelectric point: 4.75) in citrate buffer, displayed nearly neutral (0.5 mV) zeta potential. Upon loaded in ARC, SOD induced a zeta potential shift on ARC from -42 mV to -30 mV, while the neutral zeta potential of LIPO was not changed. Nearly 40% and 67 % phospholipids were lost during ARC-SOD and LIPO-SOD preparation respectively. The resultant ARC-SOD exhibited 120-180 mg/g SOD/PL ratio, comparable to that of LIPO-SOD (Table 1). In coincidence with DLS measurements, cryo-TEM images of ARC-SOD showed unilamellar and oligolamellar nanovesicles of 130 - 160 nm diameter (Fig. 1SA and 1SB).

Fluidity and order of ARC-SOD and LIPO-SOD bilayers were assessed by measuring fluorescence anisotropy (FA) and generalized polarization (GP) of the membrane probe Laurdan [34], respectively. As expected, ARC bilayers resulted more disordered (lower GP) than LIPO bilayers, displaying comparable (similar FA) fluidity (Fig. 2SA and 2SB). Upon loaded, SOD slightly increased order (without significant differences) but did not modify fluidity of ARC bilayers, suggesting some SOD partition into membranes and explaining the increase in zeta potential of ARC-SOD. Opposingly, neither fluidity not order of LIPO bilayers were affected by SOD, suggesting that SOD was not partitioned but dissolved into the inner aqueous space.

Finally, ARC-SOD retained about 100% of SOD initial activity, while for LIPO-SOD nearly 30% of the initial activity was lost during preparation.

3.2 Cytotoxicity and uptake

First, the cytotoxicity of SOD and SOD-nanovesicles on macrophages (J774A.1 cells) and enterocytes (Caco-2 cells) upon 5 and 24 h incubation, was determined by MTT assay. Upon 5 h, none of the samples [from 0.2 to 2 mM PL and from 0.8 to 8 μM proteins (SOD)] reduced cell viability (data not shown). Upon 24 h, the viability of J774A.1 was reduced only by LIPO-SOD, while the Caco-2 cells viability was slightly reduced by SOD (Fig. 1A and B).

The uptake of rhodamine-PE labelled nanovesicles by J774A.1 cells was also measured by flow cytometry along 5 h. As shown in Fig. 2, ARC was more extensively taken up than LIPO, being 6.4 folds higher at the end of 5 h.

3.3 Protective effect against oxidative damage on J774.A1 cells

Oxidative stress on J774.A1 cells was generated by H_2O_2-mediated cytotoxicity and protective effect of SOD and SOD-nanovesicles was assessed upon 5 and 24 h. As shown in Fig. 3 A and B, after 1 h incubation with 1 mM H_2O_2, the J774.A1 cells viability dropped to 50% and to 20 % 5 h and 24 h later, respectively. Upon treatments, it was found that SOD did not protect cells from H_2O_2 induced cytotoxicity. LIPO-SOD did not protect cells upon 5 h, but cell viability was enhanced to 100 % upon 24 h of incubation. In contrast, upon 5 h, cell viability was enhanced to 89 %, to be 100 % upon 24 h incubation with ARC-SOD. ARC-SOD therefore, showed the faster protective effect.

3.4 Inhibition of ROS generation and anti-inflammatory effect on macrophages stimulated with LPS

The effect of SOD and SOD-nanovesicles on ROS generation and pro-inflammatory cytokines production was determined after co-incubation with 1 μg/ml LPS for 24 h. In Fig. 4, the subcellular ROS, measured by the fluorescence of oxidized DCFDA on J774A.1 cells upon co-incubation with LPS and nanovesicles is shown. While LIPO-SOD did not and SOD slightly reduced ROS levels, ARC-SOD decreased the ROS levels by 60%. In Fig. 5 A and B, the levels of IL-6 and TNF-α induced on J774A.1 cells by LPS, respectively are shown. While SOD and LIPO-SOD did not reduce the IL-6 levels, and LIPO-SOD reduced the TNF-α levels by 37 %, ARC-SOD induced complete suppression of both cytokines.

3.5 Colloidal stability and protective effect upon digestion in SGF and SIF

Fig. 3SA and 3SB shows size, PDI and zeta potential respectively, of SOD-nanovesicles upon digestion in SGF and SIF. Major structural changes were observed upon SGF digestion: ARC-SOD and LIPO-SOD size was increased by ≈ 2 -folds; zeta potential of LIPO-SOD and ARC-SOD increased from -7 mV to ≈ 20 mV and from -30 mV to ≈ 0 mV respectively. SIF digestion did not change mean size and zeta potential of both types of SOD-nanovesicles

Fig. 6 A and B shows protective effect of SOD and SOD-nanovesicles previously digested in SGF and SIF, on J774A.1 cells pre-incubated with H_2O_2. It was found that after digested in SGF, neither SOD nor LIPO-SOD protected cells from H_2O_2 damage; in contrast ARC-SOD enhanced cell viability to 70% upon 5 h. After digested in SIF, SOD did not protect cells from toxicity induced by H_2O_2, LIPO-SOD increased cell viability up to 25 %, but ARC-SOD enhanced cell viability to 100 % upon 24 h.

Overall, SOD and LIPO-SOD lost activity upon SGF and SIF digestion, in contrast, ARC-SOD retained activity as measured by increase cell viability.

3.6 Colloidal stability at acidic pH and increasing concentrations of the bile salt NaChol

Since changes in size could be indicative of vesicles fusion or aggregation with the concomitant leakage of aqueous content or denaturation of the loaded proteins, hence colloidal stability of ARC-SOD and LIPO-SOD in acidic pH and in the presence of the bile salt sodium cholate (NaChol) was determined. Fig. 4SA and 4SB shows changes in size, PDI and zeta potential, respectively of ARC-SOD and LIPO-SOD upon incubation at pH 1, 2, 3, 4 and 5 for 1 h. ARC-SOD experienced lesser changes in size, PDI and zeta potential than LIPO-SOD. Size of LIPO-SOD increased 2- to 6- folds from pH 4 to pH 1, while the size of ARC-SOD only increased at pH 2 and pH 1. ARC-SOD and LIPO-SOD increased their zeta potential as pH decreased. Between pH 5.6 and 1, zeta potential increased from -7 to 12 mV (LIPO-SOD) and from -30 mV to -5 mV (ARC-SOD). Size changed in major extent at pH were zeta potential was

cero, at pH 2-3 for LIPO-SOD and pH ~ 1 for ARC-SOD. Most importantly, while SOD and LIPO-SOD completely lost enzymatic activity upon 1 h incubation at pH 1.2, ARC-SOD retained 31 % of enzymatic activity.

Fig. 4SC and 4SD shows changes in size, PDI and zeta potential, respectively of ARC and LIPO upon 1 h incubation at increased NaChol concentration. Changes in size of both nanovesicles only occurred at NaChol concentrations above the critical micelle concentration (CMC, 16 mM). Nonetheless, ARC experienced minor changes in size and PDI than LIPO: while LIPO size increased 3 and 10- folds, ARC size increased 2 and 3-folds at 23 mM and 113 mM NaChol, respectively. Zeta potential of LIPO and ARC was increased from -20 mV to -3 mV and from -40 mV to -15 mV, respectively, as NaChol concentration was increased from 0 to 113 mM.

In sum, the colloidal stability of ARC-SOD was higher at low pH and in presence of NaChol than that of LIPO-SOD, retaining enzymatic activity upon 1 h incubation at pH 1.2

3.7 Stability upon storage

The size, PDI, zeta potential and SOD activity of freshly prepared and stored for 5-months at 4ºC SOD-nanovesicles were determined. After 5-months the size and PDI of ARC-SOD remained unchanged, while LIPO-SOD increased ≈ 40-60 % the mean size upon 1 month of storage (from 250 nm to 400 nm) (Fig. 7). Upon 5 month of storage, only ARC-SOD retained the enzymatic activity, while LIPO-SOD reduced it by 26 % and SOD suspension complete lost enzymatic activity.

4. Discussion

Enhanced production of ROS and RNS is associated with chronic intestinal inflammation in the early stages of IBD, amplification of inflammatory process, destruction of mucosa, development of fibrosis [35] and progression of IBD [36, 37]. ROS acts as a second messenger to activate NF-κB signalling cascades leading to production of a wide spectrum of proinflammatory mediators, including TNF-α, IL-1β, NO and PGE2 [38]. Proinflammatory cytokines not only induce intestinal inflammation and associated symptoms [39, 40], but play a role in pathogenesis of the progressive and destructive forms of disease such as intestinal stenosis, bleeding, abscess, fistula formations and cancer development [41, 42]. Reducing ROS aggression thus, may well be a complementary strategy to improve the therapy of IBD.

Oral is the friendliest route of administration, leading, mostly in case of long-term therapies, to the highest adherence to treatments [43]. Compared to normal mucosa, inflamed mucosa in IBD exhibits accumulation of positively charged proteins [44]; decreased pH (5.5-2.3) [45]; increased permeability [46] and high infiltration of immune cells such as neutrophils, macrophages, lymphocytes and dendritic cells [47]. This specific environment can be used to achieve an effective SOD delivery to target cells. Here we hypothesize that oral administration of SOD loaded in suitable particulate carriers such as nanoarchaeosomes, may help to overcome the chemoenzymatic and structural barriers imposed by the GI transit, and the need of targeted intracellular activity within macrophages.

Specifically, SOD was loaded into ARC fully made of TPA from *H. tebenquichense*, a lipid mixture consisting of phosphatidylglycerophosphate methyl ester (PGP-Me), sulfated diglycosyl diphytanylglycerol diether (SDGD), phosphatidylglycerol (PG), and bisphosphatidyl glycerol (BPG) [30]. ARC display higher chemical stability than ordinary liposomes made of phospholipids. Because of the ether linkages of archaeolipids, ARC are resistant to hydrolysis; the fully saturated isoprenoid chains of archaeolipids make ARC resistant to oxidation and the *sn* 2,3 stereoisomery of archaeolipids makes ARC resistant to stereospecific phospholipases [48]. Besides, the double negatively charged PGP-Me, majoritarian polar lipid of *H. tebenquichense,* responsible for the ARC high negative zeta potential (-40 mV), is a ligand of SRA1 [21]. SRA1 is a scavenger receptor expressed mainly in macrophages and dendritic cells [49-51], with broad ligand binding properties [52]. Internalization by SRA1 lacks of negative feedback and is typically highly extensive [53]. Payload carried in ARC made of *H. tebenquichense* lipids is massively delivered to macrophages expressing SRA1, the ARC offering the additional advantage of not requiring chemical derivatization to display such targeting ligands.

In first place, we found that ARC and LIPO displayed similar protein /lipid ratio, but ~ 30 folds higher than the previously reported by [13] using liposomes of 420 nm made of HSPC: cholesterol: HSPG at 4:3:2 molar ratio. Remarkably however, LIPO-SOD manufacture required harsher conditions than ARC-SOD: the lipid film had to be hydrated and extruded at 55 - 60° C, a fact leading to the loss of ~70 % phospholipids mass and 30 % enzymatic activity during

preparation. LIPO-SOD were also more structurally labile than ARC-SOD: upon 5 month of storage, the enzymatic activity was reduced by a further 25 %, accumulating a total reduction of ~55 % enzymatic activity, besides of experiencing a significant size increase. ARC-SOD on the other hand, could be prepared at room temperature and did not lose enzymatic activity upon preparation; it exhibited negative zeta potential without requiring the addition of negatively charged lipids, and resulted of smaller size than LIPO-SOD, important factors accounting for particulate material accumulation into the inflamed mucosa [54]. Enzymatic activity and size of ARC-SOD were conserved upon 5 months of storage.

Secondly, we showed that ARC-SOD did not reduce macrophage and enterocyte viability up to 2 mM PL-8 μM SOD (2 mg/ml PL) and were highly up taken by macrophages. The safety of oral ARC made of TPA extracted from extreme halophile *Halobacterium salinarum* (up to 550 mg/kg day for 10 consecutive days in mice), have been shown several years ago [55].

In third place, despite SOD did not modify any of the three endpoints indicating antioxidant activity (cytotoxicity of H_2O_2, intracellular ROS and pro-inflammatory cytokines release), ARC-SOD reversed the H_2O_2 cytotoxicity after 5 h, decreased the intracellular ROS and completely suppressed the production of IL-6 and TNF-α on J774A.1 cells stimulated with LPS. The effect of LIPO-SOD was intermediate between those of SOD and ARC-SOD: it reverted the H_2O_2 cytotoxicity, but only upon 24 h of incubation, decreased by ~40 % the TNF-α release, but not the ROS production and IL-6 release on J774A.1 cells stimulated with LPS. If well the experimental conditions might not be comparable, Zhao et al., 2017 [15] has shown that SOD and a conjugate of SOD with O-(2-hydroxyl)propyl-3-trimethylammonium chitosan chloride of 50 KDa MW reduced by 50 % and 30% the release of TNF-α and IL-6, respectively on LPS stimulated murine peritoneal macrophages; while ROS production was only reduced by the SOD-chitosan conjugate and not by SOD. The complete inability of SOD to modify intracellular endpoints, could be owed to the fact that its activity was exerted outside instead of inside the cells. It is feasible therefore, that the highest activity of ARC-SOD would be related to its highest uptake by macrophages in comparison to LIPO-SOD, a fact responsible to a highest SOD intracellular delivery. ARC is naturally targeted to SRA1 on macrophages. SRA1 can be internalized by both clathrin- and caveolae-dependent pathways. That means that the internalized cargo by SRA1 undergoes the endo-lysosomal traffic of degradation. If well ARC are non-pH sensitive vesicles, that means that they do not release their content in response to acidic medium into cytoplasm, previously we have shown that in J774A.1 cells ARC induced more subcellular release of the highly hydrophilic polyanion pyranine from its aqueous space than LIPO [21]. These could contribute to the enhanced activity of ARC-SOD in comparison with LIPO-SOD.

In fourth place, and most importantly, we found that ARC-SOD, but not of SOD and LIPO-SOD, retained the reversion of H_2O_2 cytotoxicity after submitted to 30 min *in vitro* digestion in SGF and 2 h in SIF. These results signify that different to LIPO, ARC could protect SOD from pepsin and low pH, probably because of the protective effect of archaeolipids bilayer against the action to bile salts and pancreatic lipase degradation. In comparison the enzymatic activity of the SOD-chitosan conjugate was decreased by ~ 60% upon 2 h of treatment with pepsin and completely lost activity upon 1 h incubation at pH 2 [15]. Finally, the colloidal stability of ARC-SOD and LIPO-SOD upon incubation in SGF, SIF, acidic pH, and bile salt was assessed. ARC-SOD was less sensitive to size changes induced by acid pH than LIPO-SOD and retained 23 % of enzymatic activity upon 1 h incubation at pH 1.2. The increase in nanovesicles size at low pH is associated to leakage of encapsulated low molecular weight drugs, but not for macromolecules [56, 57]. However, denaturation of encapsulated proteins can occur if protons permeate across liposome bilayer. In such sense, we observed that LIPO-SOD completely lost enzymatic activity upon 1 h incubation at pH 1.2, whereas ARC-SOD retained enzymatic activity. This could be a consequence of the lower proton permeability of ARC membranes in comparison with LIPO membranes, due to the presence of perpendicular methyl groups in isoprenoid chains of archaeolipids [58]. On the other hand, the isoelectric point (IP) of phosphatidylcholine is close to 4 [59], a pH where electrostatic repulsion between weakly charged bilayers cannot overcome van der Waals interactions, occurring vesicle fusion and/or agglomeration [60]. The IP of archaeolipids is not known, but our results showed that it would be around pH 1. If well TPA is a mixture of lipids, where PGP-Me, the major component of the TPA, and BPG, have two, and PG has one, phosphate groups negatively charged at physiological pH, respectively. The lower IP of ARC could contribute to the higher colloidal stability to low pH than LIPO.

Size and zeta potential of ARC-SOD and LIPO-SOD did no change upon incubation in SIF. Bile salts are most important stressors for archaeosomes, where most of the entrapped markers, such as low MW carboxyfluorescein and bovine serum albumin are lost, in comparison to low pH and lipase activity [61]. The bile salt concentration in the small intestine remains relatively constant at around 5-20 mM in duodenum and jejunum and cholic acid is the major bile acid in humans [62]. Here we found that the size of ARC and LIPO was increased upon incubation with NaChol at concentrations higher than the CMC. In coincidence, Hermida et al., 2014 [63] showed that LIPO made of HSPC:cholesterol 3:2 molar ratio formed mixed vesicles of high size (1000 nm) that retained ~50% of low MW water soluble dye (pyranine) after 1h incubation with a natural bile salt extract even at 56 mM bile salt extract. At 115 mM of NaChol however, ARC was less sensitive to size changes than LIPO. The high hydrophilicity of NaChol could be responsible for the lower interaction with the higher hydrophobic archaeolipid membranes in comparison with the phospholipid membranes.

Overall, the highest resistance of ARC to low pH, simulated gastric and intestinal fluids and bile salts, could indicated that ARC-SOD thus, has higher chances of suffering less structural damage than LIPO-SOD upon oral administration

5. Conclusions

Overall, here we report novel ARC-SOD that could be prepared at room temperature and did not lose enzymatic activity upon preparation and storage, complete reversed the cytotoxicity of H_2O_2 after submitted to gastric and intestinal digestion, reduced intracellular ROS and the production of pro-inflammatory cytokines on stimulated macrophages. Because of their structural and pharmacodynamic features, ARC-SOD may be suitable for oral targeted delivery of SOD to inflamed mucosa.

Acknowledgements

The authors would like to thank to LME/LNNano for the use of electron microscopy facility and technical support. This work was supported by ANPCYT under Grant PICT 2016-4562 and Secretaria de Investigaciones Universidad Nacional de Quilmes under Grant Nanomedicinas-2. YRS, HEJ and ATC have fellowships from National Council for Scientific and Technological Research (CONICET). PS, ELR and MJM are members of the Research Career Program from CONICET.

References

1. Ng, S.C., Y.T. Lam, K.K. Tsoi, F.K. Chan, J.J. Sung, and J.C. Wu, Systematic review: the efficacy of herbal therapy in inflammatory bowel disease. Aliment Pharmacol Ther 2013, 38(8), 854-63.
2. Sanchez-Fidalgo, S., A. Cardeno, M. Sanchez-Hidalgo, M. Aparicio-Soto, I. Villegas, M.A. Rosillo, and C.A. de la Lastra, Dietary unsaponifiable fraction from extra virgin olive oil supplementation attenuates acute ulcerative colitis in mice. Eur J Pharm Sci 2013, 48(3), 572-81.
3. Rahimi, R., M.R. Shams-Ardekani, and M. Abdollahi, A review of the efficacy of traditional Iranian medicine for inflammatory bowel disease. World J Gastroenterol 2010, 16(36), 4504-14.
4. Hood, E., E. Simone, P. Wattamwar, T. Dziubla, and V. Muzykantov, Nanocarriers for vascular delivery of antioxidants. Nanomedicine (Lond) 2011, 6(7), 1257-72.
5. Greenwald, R.A., Superoxide dismutase and catalase as therapeutic agents for human diseases. A critical review. Free Radic Biol Med 1990, 8(2), 201-9.
6. Tsao, C., P. Greene, B. Odlind, and D.C. Brater, Pharmacokinetics of recombinant human superoxide dismutase in healthy volunteers. Clin Pharmacol Ther 1991, 50(6), 713-20.
7. Igarashi, R., J. Hoshino, M. Takenaga, S. Kawai, Y. Morizawa, A. Yasuda, M. Otani, and Y. Mizushima, Lecithinization of superoxide dismutase potentiates its protective effect against Forssman antiserum-induced elevation in guinea pig airway resistance. J Pharmacol Exp Ther 1992, 262(3), 1214-9.
8. Igarashi, R., J. Hoshino, A. Ochiai, Y. Morizawa, and Y. Mizushima, Lecithinized superoxide dismutase enhances its pharmacologic potency by increasing its cell membrane affinity. J Pharmacol Exp Ther 1994, 271(3), 1672-7.
9. Giri, S.N. and H.P. Misra, Fate of superoxide dismutase in mice following oral route of administration. Med Biol 1984, 62(5), 285-9.
10. Michelson, A.M. and K. Puget, Cell penetration by exogenous superoxide dismutase. Acta Physiol Scand Suppl 1980, 49267-80.
11. Huber, W., K.B. Menander-Huber, M.G. Saifer, and L.D. Williams, Bioavailability of superoxide dismutase: implications for the anti-inflammatory action mechanism of orgotein. Agents Actions Suppl 1980, 7185-95.
12. Regnault, C., M. Soursac, M. Roch-Arveiller, E. Postaire, and G. Hazebroucq, Pharmacokinetics of superoxide dismutase in rats after oral administration. Biopharm Drug Dispos 1996, 17(2), 165-74.
13. Jubeh, T.T., M. Nadler-Milbauer, Y. Barenholz, and A. Rubinstein, Local treatment of experimental colitis in the rat by negatively charged liposomes of catalase, TMN and SOD. J Drug Target 2006, 14(3), 155-63.
14. Hori, Y., J. Hoshino, C. Yamazaki, T. Sekiguchi, S. Miyauchi, S. Mizuno, and K. Horie, Effect of lecithinized-superoxide dismutase on the rat colitis model induced by dextran sulfate sodium. Jpn J Pharmacol 1997, 74(1), 99-103.
15. Zhao, N., Z. Feng, M. Shao, J. Cao, F. Wang, and C. Liu, Stability Profiles and Therapeutic Effect of Cu/Zn Superoxide Dismutase Chemically Coupled to O-Quaternary Chitosan Derivatives against Dextran Sodium Sulfate-Induced Colitis. Int J Mol Sci 2017, 18(6).
16. Suzuki, Y., T. Matsumoto, S. Okamoto, and T. Hibi, A lecithinized superoxide dismutase (PC-SOD) improves ulcerative colitis. Colorectal Dis 2008, 10(9), 931-4.
17. Corominas, M., G. Gastaminza, and T. Lobera, Hypersensitivity reactions to biological drugs. J Investig Allergol Clin Immunol 2014, 24(4), 212-25; quiz 1p following 225.
18. Sauna, Z.E., D. Lagasse, J. Pedras-Vasconcelos, B. Golding, and A.S. Rosenberg, Evaluating and Mitigating the Immunogenicity of Therapeutic Proteins. Trends Biotechnol 2018, 36(10), 1068-1084.
19. Fülöp, T., T. Mészáros, G.T. Kozma, J. Szebeni, and M. Józsi, Infusion reactions associated with the medical application of monoclonal antibodies: the role of complement activation and possibility of inhibition by factor H. Antibodies 2018, 71-9.
20. Caimi, A.T., F. Parra, M.A. de Farias, R.V. Portugal, A.P. Perez, E.L. Romero, and M.J. Morilla, Topical vaccination with super-stable ready to use nanovesicles. Colloids Surf B Biointerfaces 2017, 152114-123.

21. Altube, M.J., S.M. Selzer, M.A. de Farias, R.V. Portugal, M.J. Morilla, and E.L. Romero, Surviving nebulization-induced stress: dexamethasone in pH-sensitive archaeosomes. Nanomedicine (Lond) 2016, 11(16), 2103-17.
22. Morilla, M.J., D.M. Gomez, P. Cabral, M. Cabrera, H. Balter, M.V. Tesoriero, L. Higa, D. Roncaglia, and E.L. Romero, M cells prefer archaeosomes: an in vitro/in vivo snapshot upon oral gavage in rats. Curr Drug Deliv 2011, 8(3), 320-9.
23. Higa, L.H., H.E. Jerez, M.A. de Farias, R.V. Portugal, E.L. Romero, and M.J. Morilla, Ultra-small solid archaeolipid nanoparticles for active targeting to macrophages of the inflamed mucosa. Nanomedicine (Lond) 2017, 12(10), 1165-1175.
24. Siliakus, M.F., J. van der Oost, and S.W.M. Kengen, Adaptations of archaeal and bacterial membranes to variations in temperature, pH and pressure. Extremophiles 2017, 21(4), 651-670.
25. Altube, M.J., A. Cutro, L. Bakas, M.J. Morilla, E.A. Disalvo, and E.L. Romero, Nebulizing novel multifunctional nanonanovesicles: the impact of macrophage-targeted-pH-sensitive archaeosomes on a pulmonary surfactant. J. Mater. Chem. B. 2017, 58083-8095.
26. Parra, F.L., A.T. Caimi, M.J. Altube, D.E. Cargnelutti, M.E. Vermeulen, M.A. de Farias, R.V. Portugal, M.J. Morilla, and E.L. Romero, Make It Simple: (SR-A1+TLR7) Macrophage Targeted NANOarchaeosomes. Front Bioeng Biotechnol 2018, 6163.
27. Caimi, A.T., M.J. Altube, M.A. de Farias, R.V. Portugal, A.P. Perez, E.L. Romero, and M.J. Morilla, Novel imiquimod nanovesicles for topical vaccination. Colloids Surf B Biointerfaces 2018, 174536-543.
28. Kates, M. and S.C. Kushwaha, Isoprenoids and polar lipids of extreme halophiles, ed. S. Dassarma. 1995, New York: Cold Spring Harbor Laboratory Press.
29. Böttcher, C. and C. Pries, A rapid and sensitive sub-micro phosphorus determination. Anal. Chim. Acta 1961, 24203-204.
30. Higa, L.H., P. Schilrreff, A.P. Perez, M.A. Iriarte, D.I. Roncaglia, M.J. Morilla, and E.L. Romero, Ultradeformable archaeosomes as new topical adjuvants. Nanomedicine 2012, 8(8), 1319-28.
31. Fry, D.W., J.C. White, and I.D. Goldman, Rapid separation of low molecular weight solutes from liposomes without dilution. Anal Biochem 1978, 90(2), 809-15.
32. Zhang, X., J. Qi, Y. Lu, W. He, X. Li, and W. Wu, Biotinylated liposomes as potential carriers for the oral delivery of insulin. Nanomedicine 2014, 10(1), 167-76.
33. Sanchez-Moreno, M., M.A. Garcia-Ruiz, A. Sanchez-Navas, and M. Monteoliva, Physico-chemical characteristics of superoxide dismutase in Ascaris suum. Comp Biochem Physiol B 1989, 92(4), 737-40.
34. Harris, F.M., K.B. Best, and J.D. Bell, Use of laurdan fluorescence intensity and polarization to distinguish between changes in membrane fluidity and phospholipid order. Biochim Biophys Acta 2002, 1565(1), 123-8.
35. Alzoghaibi, M.A., Concepts of oxidative stress and antioxidant defense in Crohn's disease. World J Gastroenterol 2013, 19(39), 6540-7.
36. Pravda, J., Radical induction theory of ulcerative colitis. World J Gastroenterol 2005, 11(16), 2371-84.
37. Iborra, M., I. Moret, F. Rausell, G. Bastida, M. Aguas, E. Cerrillo, P. Nos, and B. Beltran, Role of oxidative stress and antioxidant enzymes in Crohn's disease. Biochem Soc Trans 2011, 39(4), 1102-6.
38. Schulze-Osthoff, K., M.K. Bauer, M. Vogt, and S. Wesselborg, Oxidative stress and signal transduction. Int J Vitam Nutr Res 1997, 67(5), 336-42.
39. Strober, W., I.J. Fuss, and R.S. Blumberg, The immunology of mucosal models of inflammation. Annu Rev Immunol 2002, 20495-549.
40. Ruffolo, C., M. Scarpa, D. Faggian, D. Basso, R. D'Inca, M. Plebani, G.C. Sturniolo, N. Bassi, and I. Angriman, Subclinical intestinal inflammation in patients with Crohn's disease following bowel resection: a smoldering fire. J Gastrointest Surg 2010, 14(1), 24-31.
41. Ungaro, R., S. Mehandru, P.B. Allen, L. Peyrin-Biroulet, and J.F. Colombel, Ulcerative colitis. Lancet 2017, 389(10080), 1756-1770.
42. Peyrin-Biroulet, L., E.V. Loftus, Jr., J.F. Colombel, and W.J. Sandborn, Long-term complications, extraintestinal manifestations, and mortality in adult Crohn's disease in population-based cohorts. Inflamm Bowel Dis 2011, 17(1), 471-8.

43. Choonara, B.F., Y.E. Choonara, P. Kumar, D. Bijukumar, L.C. du Toit, and V. Pillay, A review of advanced oral drug delivery technologies facilitating the protection and absorption of protein and peptide molecules. Biotechnol Adv 2014, 32(7), 1269-1282.
44. Tirosh, B., N. Khatib, Y. Barenholz, A. Nissan, and A. Rubinstein, Transferrin as a luminal target for negatively charged liposomes in the inflamed colonic mucosa. Mol Pharm 2009, 6(4), 1083-91.
45. Fallingborg, J., L.A. Christensen, B.A. Jacobsen, and S.N. Rasmussen, Very low intraluminal colonic pH in patients with active ulcerative colitis. Dig Dis Sci 1993, 38(11), 1989-93.
46. Goggins, B.J., C. Chaney, G.L. Radford-Smith, J.C. Horvat, and S. Keely, Hypoxia and Integrin-Mediated Epithelial Restitution during Mucosal Inflammation. Front Immunol 2013, 4272.
47. Antoni, L., S. Nuding, J. Wehkamp, and E.F. Stange, Intestinal barrier in inflammatory bowel disease. World J Gastroenterol 2014, 20(5), 1165-79.
48. Corcelli, A. and S. Lobasso, Characterization of lipids of halophilic Archaea, in *Methods in Microbiology—Extremophiles*, A.F. Rainey and A. Oren, Editors. 2006, Elsevier: Amsterdam. p. 585–613.
49. Naito, M., T. Kodama, A. Matsumoto, T. Doi, and K. Takahashi, Tissue distribution, intracellular localization, and in vitro expression of bovine macrophage scavenger receptors. Am J Pathol 1991, 139(6), 1411-23.
50. Naito, M., H. Suzuki, T. Mori, A. Matsumoto, T. Kodama, and K. Takahashi, Coexpression of type I and type II human macrophage scavenger receptors in macrophages of various organs and foam cells in atherosclerotic lesions. Am J Pathol 1992, 141(3), 591-9.
51. Hughes, D.A., I.P. Fraser, and S. Gordon, Murine macrophage scavenger receptor: in vivo expression and function as receptor for macrophage adhesion in lymphoid and non-lymphoid organs. Eur J Immunol 1995, 25(2), 466-73.
52. Pluddemann, A., C. Neyen, and S. Gordon, Macrophage scavenger receptors and host-derived ligands. Methods 2007, 43(3), 207-17.
53. de Winther, M.P., K.W. van Dijk, L.M. Havekes, and M.H. Hofker, Macrophage scavenger receptor class A: A multifunctional receptor in atherosclerosis. Arterioscler Thromb Vasc Biol 2000, 20(2), 290-7.
54. Lamprecht, A., U. Schafer, and C.M. Lehr, Size-dependent bioadhesion of micro- and nanoparticulate carriers to the inflamed colonic mucosa. Pharm Res 2001, 18(6), 788-93.
55. Omri, A., B.J. Agnew, and G.B. Patel, Short-term repeated-dose toxicity profile of archaeosomes administered to mice via intravenous and oral routes. Int J Toxicol 2003, 22(1), 9-23.
56. Parmentier, J., M.M. Becker, U. Heintz, and G. Fricker, Stability of liposomes containing bio-enhancers and tetraether lipids in simulated gastro-intestinal fluids. Int J Pharm 2011, 405(1-2), 210-7.
57. Hu, S., M. Niu, F. Hu, Y. Lu, J. Qi, Z. Yin, and W. Wu, Integrity and stability of oral liposomes containing bile salts studied in simulated and ex vivo gastrointestinal media. Int J Pharm 2013, 441(1-2), 693-700.
58. Yamauchi, K., K. Doi, Y. Yoshida, and M. Kinoshita, Archaebacterial lipids: highly proton-impermeable membranes from 1,2-diphytanyl-sn-glycero-3-phosphocholine. Biochim Biophys Acta 1993, 1146(2), 178-82.
59. Petelska, A.D. and Z.A. Figaszewski, Effect of pH on the interfacial tension of lipid bilayer membrane. Biophys J 2000, 78(2), 812-7.
60. Nacka, F., M. Cansell, J.P. Gouygou, C. Gerbeaud, P. Meleard, and B. Entressangles, Physical and chemical stability of marine lipid-based liposomes under acid conditions. Colloids Surf B Biointerfaces 2001, 20(3), 257-266.
61. Patel, G.B., B.J. Agnew, L. Deschatelets, L.P. Fleming, and G.D. Sprott, In vitro assessment of archaeosome stability for developing oral delivery systems. Int J Pharm 2000, 194(1), 39-49.
62. Kararli, T.T., Comparison of the gastrointestinal anatomy, physiology, and biochemistry of humans and commonly used laboratory animals. Biopharm Drug Dispos 1995, 16(5), 351-80.

63. Hermida, L.G., M. Sabes-Xamani, and R. Barnadas-Rodriguez, Characteristics and behaviour of liposomes when incubated with natural bile salt extract: implications for their use as oral drug delivery systems. Soft Matter 2014, 10(35), 6677-85.

Figure captions

Fig. 1 Cell viability upon 24 h incubation with SOD (8 μM proteins), LIPO-SOD (2 mM PL-8 μM proteins) and ARC-SOD (2 mM PL-8 μM proteins) evaluated by MTT on (A) J774A.1 and (B) Caco-2 cells. (n=3 batches). Kruskal-Wallis multiple comparisons test. Asterisks indicate significant differences between groups and control.

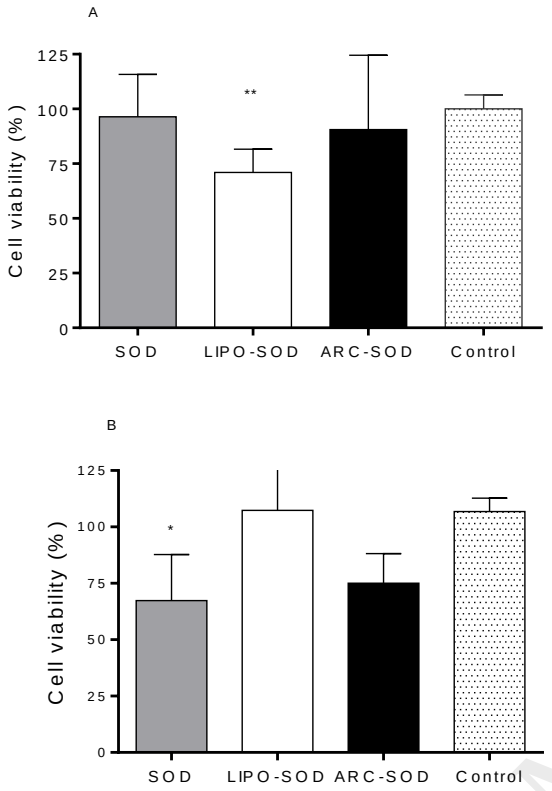

Fig. 2 *In vitro* cellular uptake. RhPE fluorescence intensity (FI) of J447A.1 cells after 1 and 5 hours of incubation with RhPE labelled nanovesicles. (n=3).

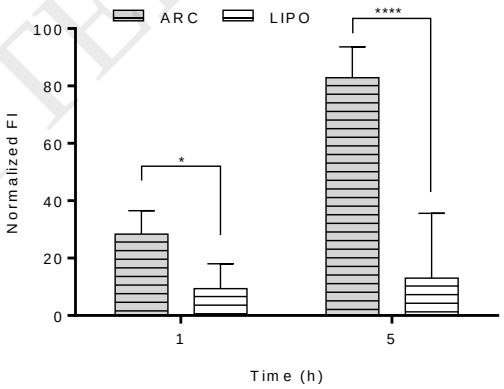

Fig. 3 Effect of SOD, LIPO-SOD and ARC-SOD on oxidized J774.A1 cells upon 5 h (A) and 24 h (B) of incubation. Controls cells incubated with medium. (n=3). Dunnett's multiple comparisons test. Asterisks indicate significant differences between groups and H_2O_2.

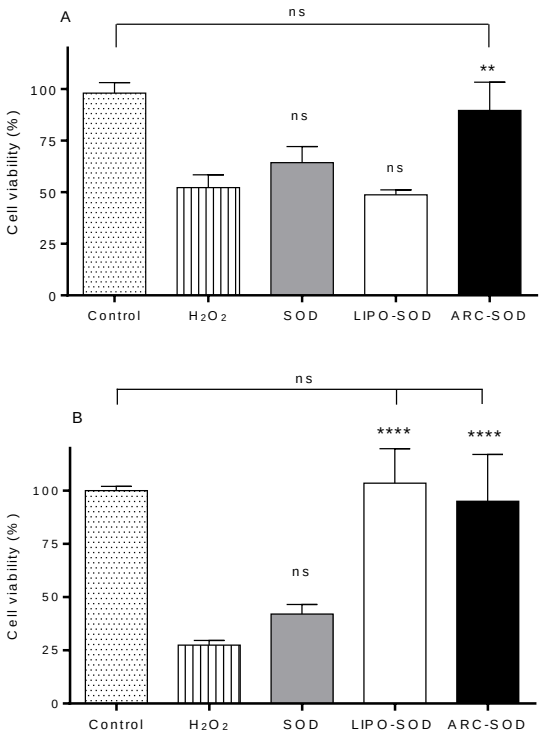

Fig. 4 Decreased generation of reactive oxygen species (ROS). Fluorescence intensity of carboxy-DCFDA on J774A.1 cells after 24 h coincubation with LPS (1 µg/ml) and SOD, LIPO-SOD or ARC-SOD. (n=2).

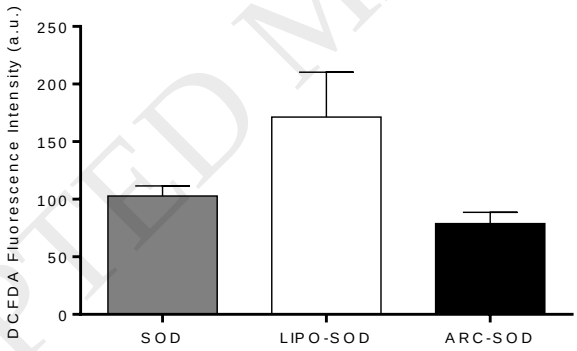

Fig. 5 *In vitro* anti-inflammatory activity. Proinflammatory cytokines (A) IL-6 and (B) TNF-α released by J774A.1 cells where measured upon 24 h of coincubation with LPS (1 µg/ml) with SOD, LIPO-SOD or ARC-SOD. (n=3). Dunnett's multiple comparisons test. Asterisks indicate significant differences between groups and LPS.

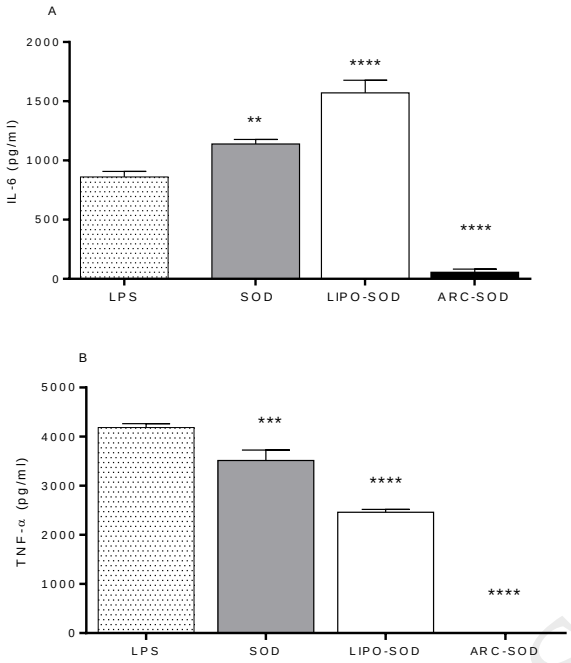

Fig. 6 *In vitro* activity of digested samples with simulated gastric fluid for 5 h (A) and simulated intestinal fluid for 24 h (B) express as cell viability of J774A.1. Dunnett's multiple comparisons test. Asterisks indicate significant differences between groups and H_2O_2.

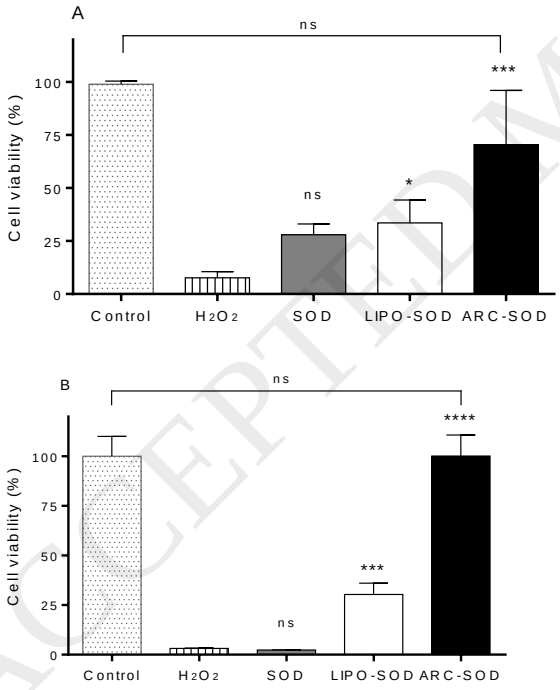

Fig. 7 Colloidal stability upon storage. Size and polydispersity index of nanovesicles freshly prepared (0) and after 5 months of storage at 4ºC. PDI: Polydispersity Index. Tukey's multiple comparisons test.

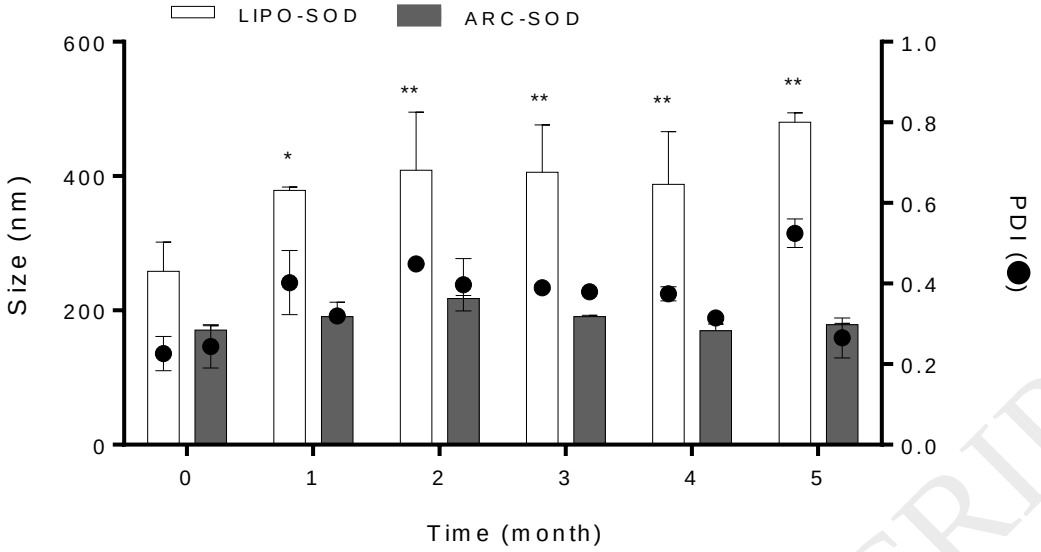

Table 1. Structural characterization of nanovesicles

Table 1.

Formulation	Mean size nm ± SD (PDI ± SD)	Z potencial (mV ± SD)	Phospholipids (mg/ml ± SD)	Protein (mg/ml ± SD)	Encapsulation Efficiency (%)	Activity (%I /mg protein)
ARC	186 ± 30 (0.22 ± 0.04)	-42.3 ± 2.7	19.1 ± 4.4	-		-
ARC-SOD	171 ± 14 (0.229 ± 0.060)	-30.4 ± 3.9	11.6 ± 3.6	1.35 ± 0.44	34 ± 9	74
LIPO	273 ± 43 (0.273 ± 0.17)	-5.9 ± 1.9	12.0 ± 5.7	-		-
LIPO-SOD	259 ± 49 (0.389 ± 0.14)	-7.4 ± 2.2	6.7 ± 3.1	1.22 ± 0.70	30 ± 17	54

Data are express as mean ± SD of 5 different batches. SD: standard deviation. PDI: polydispersity index